COMPUTATIONAL EVALUATION OF MECHANISTIC PATHWAYS OF ACTION OF SUPEROXIDE DISMUTASE

By

Shambhavi Velishala

Submitted in partial Fulfillment of the Requirements

for the Degree of

Master of Science

in the

Chemistry

Program

YOUNGSTOWN STATE UNIVERSTIY

DECEMBER, 2012.

COMPUTATIONAL EVALUATION OF MECHANISTIC PATHWAYS OF ACTION OF SUPEROXIDE DISMUTASE

Shambhavi Velishala

Signature:

Shambhavi Velishala, Student Date

Approvals:

Dr. Howard Mettee, Thesis Advisor Date

Dr. Ganesaratnam K. Balendiran, Committee Member Date

Dr. Sherri Lovelace-Cameron, Committee Member Date

Peter J. Kasvinsky, Dean of School of Graduate Studies and Research Date

ABSTRACT

Computational studies on thermodynamics of dismutation of superoxide anion radicals (O_2^-) to hydrogen peroxide and molecular oxygen was conducted with various theoretical models using a variety of basis sets. The computational models include semi-empirical, Hartree-Fock and density functional contained in the Spartan 2004* program suite. The catalytic role of Cu^{2+} in the superoxide dismutase enzyme was reflected by observing its effect on reducing the activation energies. Activation energies were computed for various transition states complex involved in concerted, two step and three step mechanisms catalyzed by $[Cu(NH_3)_4(H_2O)_2]^{2+}$. Based on this analysis, mechanisms which include the peroxy radical ($^{\cdot}OOH$) are less favored than those which include neutral O_2 in a transition state complex, or involve both H^+ donors and a superoxide (O_2^-) in a single step.

ACKNOWLEDGEMENTS

I would like to express my sincere gratitude to my advisor Dr. Howard Mettee for his continuous support and guidance during my research. His guidance helped me in all the aspects of my research and writing of this thesis. Besides my advisor, I would like to thank my committee members Dr. Ganesaratnam K Balediran and Sherri Love-lace Cameron for their insightful comments and advises on my thesis.

My sincere thanks go to Department of Chemistry and Graduate School of Studies for all the financial support. Last but not least I'm grateful to my family members and friends for their support and blessings.

TABLE OF CONTENTS

LIST OF TABLES

LIST OF FIGURES

LIST OF SYMBOLS AND ABBREVIATIONS

AM1	Austin model 1, a semi-empirical method
B3LYP	A density functional method due to Lee, Yang and Parr
DFT	Density functional theory
HF	Hartree-Fock method
LDA	Local density approximation
MNDO	Modified neglect of diatomic overlap
PM3	Parameterized model 3, a semi-empirical method
ΔG^0	Standard free energy change
ΔH^0	Standard enthalpy change
ΔS^0	Standard entropy change
R	Universal gas constant
k	Boltzmann constant
STO-3G	Slater type orbitals in terms of three Gaussians
6-31G*	Split valence basis set with d-orbitals
6-31G**	Split valence basis set with additional p-orbitals
PAW	Projector augmented-wave method (density functional method)

1. INTRODUCTION

The use of modern molecular modeling techniques to study the internal dynamics of chemical reactions has become increasingly possible due to the advances in the capacity and sophistication of today's computers and software[1]. It is important to find a practical compromise between the level of the computational model and the time required to achieve the desired degree of accuracy. Secondly, it is important to understand the mechanism of enzyme action in biological systems in order to influence pathways that have been altered by toxic agents. This project is presented as a series to compute both thermodynamic ground state properties of reactants and products, as well as transition state energetic, in order to distinguish favorable mechanistic pathways. Enzymatically active sites can in many cases be described with clarity and understanding, while solid state and extended network systems are less simply treated.

Superoxide dismutase (SOD) is one of the most important enzymes in the front line of defense against oxidative stress in mammalian tissues, plants, blood, algae and aerobic bacteria[2,3]. It catalyzes the decomposition of the toxic superoxide ion radical, O_2^-, which is a product of numerous metabolic oxidative pathways. It involves in the dismutation of superoxide into oxygen and hydrogen peroxide.

$$2O_2^- + 2H^+ \xrightarrow{\text{SOD}} O_2 + H_2O_2 \qquad [1]$$

Catalase then continues to remove the hydrogen peroxide in a further reaction.

$$2H_2O_2 \xrightarrow{\text{Catalase}} 2H_2O + O_2 \qquad [2]$$

It has been found that SOD is an anti-inflammatory agent in animal cells that inhibits the peroxidation of fatty acids in inflammation and hemostasis. It is involved in anti- aging and anti cancer processes[4, 5]. SOD is used to treat arthritis and ulcers and it suppresses the effects of long exposure to radiation and smoke. Because of the theoretical difficulty of treating free protons H^+, and their likely stabilization of water as H_3O^+ or other bases in chemical systems, a more convenient representation of the SOD reaction is as follows.

$$2O_2^- + 2H_3O^+ \xrightarrow{\text{SOD}} H_2O_2 + 2H_2O + O_2 \qquad [3]$$

There have been some published attempts to understand the role of superoxide dismutase in the above overall reaction, seeking in particular the significance of the cuprous and cupric ions Cu (I) and Cu (II). These studies focused mainly on two generally accepted possible mechanisms[7].

Mechanism 1:

$$Cu^{2+} + O_2^- \rightarrow Cu^+ + O_2 \qquad [4]$$

$$Cu^{2+} + O_2^- + 2H^+ \rightarrow Cu^{2+} + H_2O_2 \qquad [5]$$

Mechanism 2:

$$Cu^{2+} + O_2^- \rightarrow (CuO_2)^+ \qquad [6]$$

$$(CuO_2)^+ + O_2^- \rightarrow (CuO_2) + O_2 \qquad [7]$$

$$(CuO_2) + 2H^+ \rightarrow Cu^{2+} + H_2O_2 \qquad [8]$$

The present project is an attempt to distinguish between these mechanistic choices, as well as two other possibilities using computational methods. Computational modeling theory places the copper ion in an active site accessible to O_2^- and H^+ donors, ligated into position by four coplanar histidine rings, modeled as four coordinated ammonia or imidazole molecules for example $[Cu(NH_3)_4(H2O)_2]^{2+}$. Then, the thermodynamic properties of the reactants and products of each mechanistic step are calculated, along with those of the activated complex (transition state) between them. These results in turn are used to form an energy profile for each mechanism to distinguish their relative importance.

1.1 MODELING INTRODUCTION

This project uses molecular structures constructed using the Spartan 2004* suite of programs accessible from Wavefunction, Inc. The theoretical methods and type of basis sets include semi-empirical (PM3), Hartree-Fock (HF-6-31G*) and density functional (DF-6-31G*) in this package. Dell OPTIPLEX GX-270 desktop computers were used throughout the work. These methods have their origins in the Schrodinger equation, which calculates the energy in a system of repulsive and attractive interactions found in typical molecules, but the precise mathematical description of the Hamiltonian operators and actual eigenfunctions need not be written by the program user, as they are incorporated into the modeling software. It is usually enough to form the molecules or radicals/ions structurally by using ordinary chemical bonding geometries, and then to identify the method and a form of orbital approximation (basis set), multiplicity, etc and finally to compute the corresponding energies, enthalpies and entropies for each molecular species.

For a given molecule or ion, molecular mechanics is usually used first to find the most stable configuration of established bond lengths, bond angles and strengths. Here the atoms are joined by springs of various force constants. This is the most primitive form of theory since there are no provisions to account for separate nuclei and electrons, only their shared behavior as polarizable atoms. The semi-empirical and Hartree-Fock methods use molecular orbitals (MOS) made up of atomic orbitals on each nuclear centre, but density functional methods do not use MOS to explain the electron distribution. They use a density gradient and the shapes of HF orbitals to produce a "density functional", formed around the nuclear framework. Finally, for the total molecule Moller-Plesset or coupled clusters methods combine the excited state and ground state configurations to account for electron-electron correlation that is not treated in the HF method.

In each method of investigation, the modeling procedure is the same. The molecule is formed atom by atom, the positions being prompted by the program and the modeler's input. Then a selection of method and the basis set is made along with the desired properties to be computed and the calculation is started. When convergence of the energy is reached in an energy minimization, the additional properties can then be calculated (vibrational frequencies for example). Finally the results are analyzed, in terms of their thermodynamic properties and equilibrium geometries.

1.2 ENZYMATIC ACTIVE SITE

Copper-zinc superoxide dismutase is a dimeric enzyme consisting copper and zinc ions in each subunit, and there are two active sites in each subunit (Fig 1). The copper ion is surrounded by four histidine residues in a distorted square planar geometry. One residue acts as a bridge between the zinc and copper ions. An aspartate and two other

histidine residues complete the coordination of the zinc ion. The catalytic copper ion is placed at the bottom of a shallow protein cavity, which has several charged residues on its surface which are believed to play a role in steering the charged superoxide (O_2^-) to the copper ion. The zinc ion is totally buried in the protein.

Figure 1 displays the electrostatic potential of Cu-Zn superoxide dismutase by MCRee et al[19]. Red contours represent negative electrostatic potential and blue contours denote positive electro static potentials. At the top left and bottom right two active sites are found in each dimer, one in each lobe[19]. A significant concentration of positive electrostatic potential was formed due to steering effects, which help to place the superoxide anion closer to the copper ion.

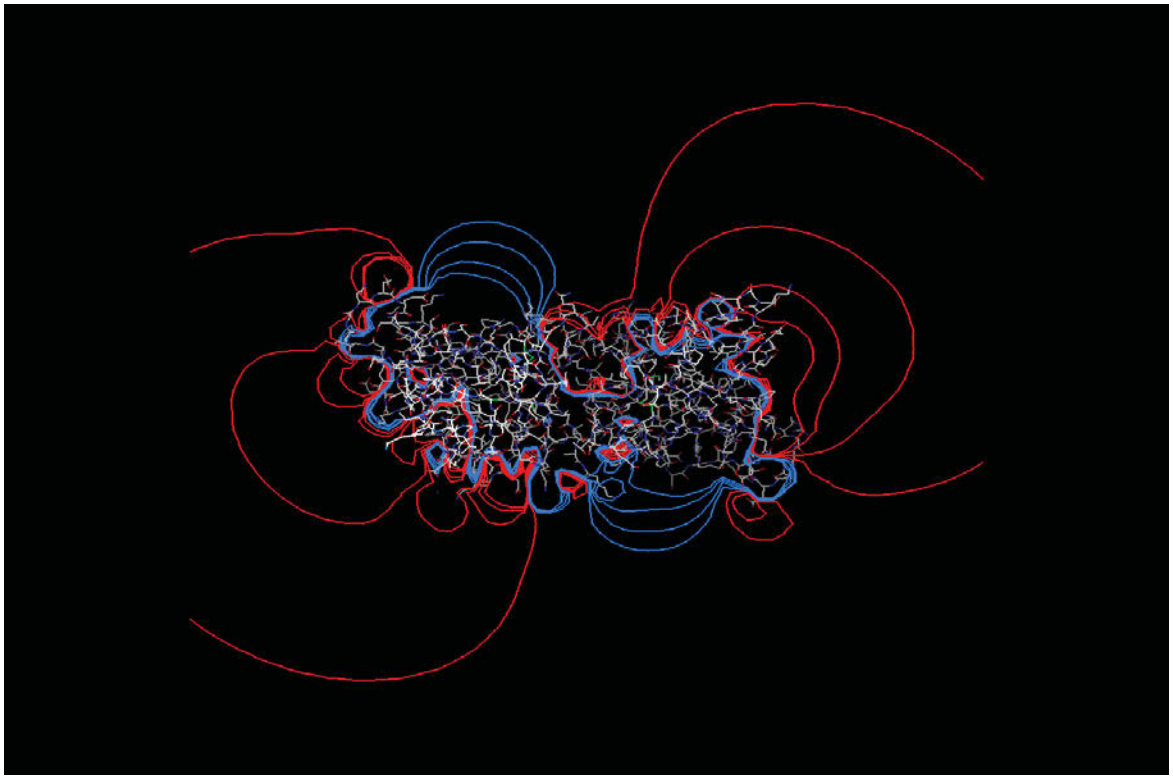

Figure 1 Two active sites in SOD[19]

1.3 MECHANISMS

Two mechanisms have been proposed in the literature for the dismutation reaction. In the most widely accepted mechanism[7], copper ion is repetitively oxidized and reduced in a two step cyclic process. In the first step, the superoxide ion itself is oxidized by giving its electron to copper, and forming molecular oxygen equation [9]. In the second step, a second superoxide is condensed by simultaneously accepting an electron, from the now reduced copper, and two protons to form hydrogen peroxide, as in equation [10].

$$Cu^{2+} + O_2^- \rightarrow Cu^+ + O_2 \qquad [9]$$

$$Cu^+ + O_2^- + 2H^+ \rightarrow Cu^{2+} + H_2O_2 \qquad [10]$$

Within this concept, it has been recommended that the bond between copper and the His61 (histidine, HI^+, modeled as imidazole) breaks down losing a H^+ in the first step, forming a very basic imidazolate group (I), which would in turn receive a proton from either hydronium or water. In the second step, the H^+ is transferred from the His61 to the second superoxide molecule, to form an intermediate free peroxide radical, $HO_2^{\cdot}$ equation [12]. The Zn ion helps position the HI^+.

$$Zn\text{--}HI^{+}\text{--}\ Cu^{2+} + O_2^{-} \longrightarrow Zn\text{--}I + O_2 + Cu^{+} + H^{+} \quad [11]$$

$$O_2^{-} + H^{+} \longrightarrow HO_2^{\cdot} \quad [12]$$

$$Cu^{+} + H^{+} + HO_2^{\cdot} \longrightarrow Cu^{2+} + H_2O_2 \quad [13]$$

$$Zn\text{--}I + Cu^{2+} + H_3O^{+} \longrightarrow Zn\text{--}HI^{+}\text{--}\ Cu^{2+} + H_2O \quad [14]$$

Parallel to the second step, the His61 must choose another H^{+} from either hydronium or water in order to re-establish the bridge between zinc and copper, and to be prepared to lose this proton again, in the following step equation [14]. On the basis of quantum mechanical calculations, Osman, Bash and Rosi[9,10] proposed another mechanism. They recommended the formation of a stable copper-superoxide intermediate complex that is capable of oxidizing a second superoxide to form oxygen. In this case no breaking of copper-His61 bond takes place, and a neutral (CuO_2) complex is presented.

$$Cu^{2+} + O_2^{-} \rightarrow (CuO_2)^{+} \quad [15]$$

$$(CuO_2)^{+} + O_2^{-} \rightarrow (CuO_2) + O_2 \quad [16]$$

$$(CuO_2) + 2H^{+} \rightarrow Cu^{2+} + H_2O_2 \quad [17]$$

The source of the two H^{+} in the last step of the second mechanism forming hydrogen peroxide is not specified. We chose to model primitive transition states at first by using the principal reactants including Cu^{2+}, $2H^{+}$ and $2O_2^{-}$, where Cu^{2+} is an electron transfer agent to oxidize one superoxide and condense $2H^{+}$ with O^{2-} to form H_2O_2 equation [13]. The symbols Cu^{2+} and Cu^{+} refer to octahedral complex [Cu

$(NH_3)_4(H_2O)_2]^{2+}$, and the tetrahedral complex [Cu $(NH_3)_3(H_2O)]^+$ where the NH_3 molecules mimic the approximately co-planar histidine in the active site ligating the copper ion. This simplifying substitution does not significantly affect the net energy change for the reaction (ΔH_{rxn} = - 637.2 kJ/mol). According to theory[7], one of the NH_3 ligands separates in first reduction step, and reunites later. Then, we looked for the minimum energy pathway in the mechanistic schemes to determine the most reasonable mechanism for the overall catalyzed reaction equation [18].

$$2O_2^- + 2H^+ \xrightarrow{Cu^{2+}} O_2 + H_2O_2 \qquad [18]$$

1. 4 THERMODYNAMICS

As a criterion of the ability of theory to predict the experimental values, we chose to calculate the thermodynamic parameters of the dismutation reaction [19], where the donor of H^+ was H_3O^+, since the energy of the bare H^+ is difficult to evaluate without an electronic framework.

$$2\ H_3O^+ + 2O_2^- \longrightarrow H_2O_2 + O_2 + 2H_2O \qquad [19]$$

Gas phase values for standard entropies and for the enthalpies of formation at 298 K are presented from the JANAF- NIST Thermodynamic Tables, [22] published in 1998. Whether a given theoretical model was possible or not, in the first instance, could be checked by comparing its overall predictions with those based on the experimental values.

	H_3O^+	O_2^-	O_2	H_2O_2	H_2O (v)
ΔH_f^o (KJ/mol):	581.6	-48.593	0.00	-136.106	-241.826
S^o (J/K mol):	192.257	209.591	205.147	232.991	188.834

Using the standard Gibbs equation $\Delta G = \Delta H - T\Delta S$ for the reaction [19] and converting to cal/kcal, we have

ΔH_{rxn} = -402.50 kcal/mol ΔS_{rxn} = 0.00279 kcal/mol ΔG_{rxn} = -403.57 kcal/ mol

It's clear that this reaction has a great thermodynamic driving force, mainly resulting from the electrostatic attractions of the oppositely charged ions and the consequent rebonding of the protons from H_3O^+ to form H_2O_2. The solvent effects in actual reactions would include greater stabilization of the charged species, but these energies are usually less than those involved in chemical bonds themselves.

2. COMPUTATIONAL METHODS

2.1 INTRODUCTION

The overall chemical reaction that forms the basis for the present molecular modeling calculations contain the superoxide and acid reactants, and oxygen, hydrogen peroxide and water as products in their thermodynamic ground states at 298K and 1 bar.

$$2O_2^- + 2H_3O^+ \xrightarrow{SOD} H_2O_2 + 2H_2O + O_2 \qquad [20]$$

According to thermodynamic theory, the driving force for the reaction is not concerned with transition state energies of intermediates. In the usual approach enthalpies (ΔH's) and absolute entropies (S's) for the individual molecules are computed by specifying the type of calculation (Semi-empirical, Density functional, Hartree-Fock, etc) and the different basis sets of orbitals (PM3, 6-31G* etc) required to calculate ΔH, ΔS, and ΔG for a given reaction. The program finds the equilibrium molecular geometry by changing the bond lengths and bond angles and calculating the energy at each configuration, and choosing the lowest energy structure. At this geometry the thermodynamic parameters (ΔH_f for PM3, and electronic energy E^0 and H^0 for SCF and DF, and absolute S^0 for all the three models) are computed from the moments of inertia, the normal vibrational modes and most importantly the electronic energy of all the electrons attracted to the frozen nuclear skeleton.

These thermodynamic parameters are independent of mechanistic pathway connecting reactants and products. Even though biological systems containing proteins (enzymes) contain numerous potential H^+ donors including H_2O, these are commonly

modeled as H_3O^+ realizing they could be another. $HArg^+$ is taken for SOD in the step, and $HHis^+$ (histidine) is another possibility. Using the suggestion of Osman and Bach[9,10] we adopt the $HArg^+$.

The proposed two step and three step mechanisms actually involve additional composite groups containing zinc ion and protein. However, the active site includes copper ion which plays the most significant redox catalytic role. The energy and configuration of the transition states were minimized at an energy maximum between the initial and final state. The Cu^{2+} is octahedrally complexed with six ligands including $4NH_3$ and $2H_2O$ molecules. The NH_3 molecules mimic the imidazole rings in the active site which suspend the Cu^{2+}. The H_2O molecule is replaced by the O_2 or $^{\cdot}OOH$ peroxy radical depending up on the mechanism. The Cu^+ is tetrahedrally complexed with O_2, OOH, or H_2O and NH_3. In this method the electron transfer role of Cu^{2+} was included without any difficulty of a particular active site transition state in the proposed mechanisms. We calculated the activation energies based on the energy differences between initial and transition states as is traditional.

2.2 SEMI-EMPIRICAL METHODS

Austin Model One (AM1)[11] and parameterized Model Three (PM3)[12] are the most commonly used semi-empirical methods. Semi-empirical models follow directly from *ab initio* molecular orbital theories (Hartree-Fock). These theories are based on the simplifications that measure only the valence electrons in the calculations, ignoring the inner shell electrons ($1s^2$ etc) which are regarded as a part of a fixed core. Only a minimum set of valence orbitals are measured on each atom [e.g. 1s (core) + 2s, $2p_x$, $2p_y$, $2p_z$ (valence orbitals on carbon)]. These are two of the quantum chemical methods which

result from the Schrodinger equation, where the molecules are treated as a group of frozen nuclei and electrons. The hypothesis is made in these semi-empirical methods that the atomic orbitals forming on different atoms do not overlap, which is considered the central approximation. The AM1 and PM3 models include similar approximations but they differ in their parameterization of the exponential functions used to compose atomic orbitals.

The parameterization of atomic orbital constants was done to reproduce a wide variety of experimental data. These adjustable parameters were selected to give known equilibrium geometries, ionization potentials, heats of formation and dipole moments of well known compounds. These parameters are multipliers and exponents of the Gaussian functions used to represent the atomic orbitals. Semi-empirical methods reduce the computation effort directly from the fourth power of the total number of basis functions (in *ab intio* models) to the square of the number of the basis functions. The key approximation, termed as NDDO (neglect of diatomic differential overlap) approximation, reduces the number of electron-electron interactions, and eliminates overlap of atomic basis functions on adjacent as well as different atoms ignoring bonding effects. Innermost atomic shells (1s for second row C, O and N atoms) are kept frozen in order to speed up the computation time. The frozen core orbitals (CO), are expressed in an auxiliary group of Slater-type basis functions. AM1 and PM3 are the extensions to the MNDO method, which means Modified Neglect of Diatomic overlap. Diatomic overlap takes place on only adjacent atomic centers, containing bonding interactions. The semi-empirical calculations constantly use basis sets containing Slater- type s, p and d orbitals. Semi-empirical models play a key role in structure determination and agree with good

experimental data over a wide range (bond angles from a normal 130^{o} to an approximately linear 170^{o} and bond distances in between 0.1 and 0.3 nm). The earlier AM1 is characterized only for the four atoms like H, C, N and O, the so called "organic" elements. PM3 has advantage over AM1 in that it is parameterized for more atoms, containing third row non metals, aluminum and halogens. To measure molecular properties PM3 model has been widely used and was extended recently to measure transition metals. Two Gaussian functions are used for the core repulsion in PM3, whereas AM1 uses a variable number between one and four Gaussian per element. AM1 and PM3 give slightly different numerical values, and they are both parameterized to give the energies of molecules in the form of standard enthalpies of formation and entropies (relative to the elements set to zero at 298 K and 1 bar for the enthalpy and set to zero at 0 K for the entropy of elements and compounds). This differs from the Hartree-Fock models, which gives total energy E_{tot} at 0K (where the zero energy state is referred as a frozen nuclear frame work separated from all the electrons).

The AM1 model was developed to reduce the problems with MNDO, which were the inability to produce steric interference and hydrogen bonding. This method was designed to modify the term core-core by using Gaussian functions. AM1 deals with repulsion by a core repulsion function (CRF), an additional Gaussian function, for any pair of atoms XY in the molecule. Z_X and Z_Y refer to the nuclear charges on atoms X and Y. γ_{XY} refers to electron repulsion integrals.

$$CRF\ (XY) \quad = \quad Z_X Z_Y \gamma_{XY} [1+F\ (X) + F\ (B)] \qquad [20]$$

$$F\ (X) = \exp\ (-\alpha_X R_{XY}) \quad + \quad \sum_I K_{Xi} \exp\ [L_{Xi} (R_{XY} - M_{Xi})^2] \qquad [21]$$

$$F\ (Y) = \exp\ (-\alpha_Y R_{XY}) \quad + \quad \sum_J K_{Yj} \exp\ [L_{Yj} (R_{XY} - M_{Yj})^2] \qquad [22]$$

Where α, L, K and M are empirically adjustable parameters.

Excessive interatomic repulsions were reduced in two ways. First, one or more Gaussians were added to the system to reduce larger internuclear separations. Secondly, repulsive Gaussians were added to reduce the smaller internuclear separations.

MNDO is a semi-empirical method containing Gaussian functions as in AM1 and PM3. MNDO is used to characterize the valence electrons of closed-shell molecules. These electrons move towards the inner-shell electrons and into the field of fixed core potentials of the nuclei.

$$\Psi_i = \sum_V C_{Vi} \Phi_v \qquad [23]$$

From Roothan-Hall equations C_{Vi} coefficients are found (the variation method). Then the equation was expressed in the form of:

$$\sum_v (F_{\mu v} - E_i \delta_{\mu v}) = 0 \qquad [24]$$

Where E_i are the eigenvalues and the $\delta_{\mu v}$ is the Kronecker δ. The elements of Fock matrix, $F_{\mu v,}$ are the sum of a one electron part $H_{\mu v}$ (core Hamiltonian) and a two-electron part $G_{\mu v}$. Therefore it is represented by the following

$$F_{\mu v} \quad = \quad H_{\mu v +} G_{\mu v} \qquad [25]$$

The electronic energy E_{el} is given by:

$$E_{el} = \frac{1}{2} \sum_{\mu} \sum_{\nu} P_{\mu\nu} (H_{\mu\nu} + F_{\mu\nu}) \quad [26]$$

Where, $P_{\mu\nu}$ accounts for bond order matrix.

The Fock matrix has the following six terms:

1) One-center one-electron energies $U_{\mu\nu}$, which are the sum of kinetic and potential energies and are expressed by

$$U_{\mu\nu} = (\partial^2 \Phi_{\mu} / \partial \tau_1) - (e^2 / r_1) \Phi_{\mu} \, d\tau \quad [27]$$

2) One-center two-electron repulsion integrals, i.e., repulsive coulomb integrals were represented by

$$(\mu\mu, \nu\nu) = g_{\mu\nu} \quad [28]$$

Where μ, ν are atomic orbitals (basis functions)

3) One atom exchange integrals were expressed by

$$(\mu\nu , \mu\nu) = h_{\mu\nu} \quad [29]$$

4) Two-centre one-electron core resonance integrals $\beta_{\mu\lambda}$ which have the following form

$$\beta_{\mu\lambda} = \int \Phi_{\mu}(e^2 / r_B) \Phi_{\lambda} \, d\tau_{\lambda} \quad [30]$$

5) Two-center, one electron attractions $V_{\mu\nu,B}$ between an electron in the distribution core of atom B and the $\psi_{\mu} \psi_{\nu}$ on atom A.

6) Two-center two-electron repulsion integrals (μν, λσ) represent the energy of interaction between the charge distribution at atom A and atom B using functions μ and ν on atom A and λ, σ on B.

$$(\mu\nu, \lambda\sigma) = \int\int \Phi_\mu^{*(1)} \Phi\nu^{(1)} [1/ r_{12}] \Phi\lambda^{*(2)} \Phi\sigma^{(2)} d\tau_1 d\tau_2 \quad [31]$$

The total energy E_{tot} is the summation of electronic energy $_{Eel}$ and the repulsions between the cores of atoms A and B (E_{AB}^{core}).

$$E_{tot}^{mol} = E_{el} + \sum_A \sum_B E_{AB}^{core} \quad [32]$$

The heat of formation of the molecule is calculated from its total energy by subtracting the added experimental heats of formation of the atoms and the electronic energies in the molecule.

$$\Delta H_f^{mol} = E_{tot}^{mol} - \sum_A E_{el}^{A} + \sum_A \Delta H_f^{A} \quad [33]$$

From restricted single-determinantal wave functions the electronic energies were calculated by using the same approximations and parameters as in molecular NDDO calculations.

2.3 HARTREE-FOCK (HF) OR *AB INITIO* MODEL

Hartree-Fock (HF) or *ab initio* model is a type of approximation that determines the ground state energy and ground state wave function of a many quantum body systems. This approximation is the best method to calculate the true many electron wave functions of atoms and molecules which are a product of N single electron wave functions, in determinant form [34].

$$\Psi(1, 2, 3\ldots\ldots N) = 1/\sqrt{N}! \begin{vmatrix} K_1(1)\, K_2(2)\ldots\ldots K_n(1) \\ K_1(1)\, K2(2)\ldots\ldots K_n(2) \\ K_1(n)\, K_2(n)\ldots\ldots K_n(N) \end{vmatrix}$$

The K's are spin orbitals and $1/\sqrt{N}!$ is a normalizing factor. Hartree-Fock wave functions and energies of the system are obtained by the variation method, which minimizes the energy with respect to the coefficients of the orbitals. It is based on the Born-Oppenheimer approximation, which states that nuclear motion including vibrational and rotational components are independent of electronic motion. Furthermore, it states that on the time scale of electronic motion, the nuclei are frozen in their equilibrium states. Slater type orbitals (STO) are usually used to characterize atomic orbitals in the Hartree-Fock model, and they are expressed in exponential form.

$$S_{n,I,m} = N_{(n.I)}\, r^{n-1}\, e^{\zeta r}\, Y_m(\theta,\varphi) \qquad [35]$$

$Y_m(\theta,\varphi)$ denote spherical harmonics and ζ is the adjustable parameter. By using a linear combination of one to six Gaussian type orbitals, each STO is expressed by terms of the following type.

$$\Phi(r) = (2\alpha / \pi)^{3/4}\, e^{-\alpha\, r**2} \qquad [36]$$

Many electron-wave functions can be approximated by a multiplication of many one-electron-functions, followed by an assumption which is part of the HF approximation theory. The assumption is that the electronic solutions for a many electron molecule are similar to a combination of one-electronic energy solutions for the hydrogen atom.

Various basis sets are normally recommended, depending upon the computer resources of the system, to obtain desired accuracy.

2.4 HARTREE-FOCK WAVE FUNCTION AND BASIS SETS

Closed-shell and Open-shell wave functions:[13]

Closed-shell single determinant wave functions (all electrons paired into spatial orbitals) describe the most common form of HF theory, and they are accurate in describing the ground state properties of most molecules with an even number of electrons. Open shell single determinant wave functions describe systems with an even number of electrons (triplets and excited states), as well as odd number of electron systems (radicals) distinguished by electronic states other than closed-shell singlet states.

STO-3G minimal basis sets:[14]

The basis set Slater Type Orbital STO-3G contains minimal basis Slater type orbitals and develops each one in terms of three Gaussian functions. Calculations of Slater type orbitals containing the exp (-r) term are very time consuming and mathematically difficult to perform and to evaluate two electron integrals. Evaluation can be done analytically using Gaussian functions due to the exp ($-r^2$) term, which is not present in the explicit Slater type orbitals. STO-3G basis sets should be noted to contain two features of Gaussian expansions. First, the Slater 2s, 3s, 4s and 5s functions are developed in terms of the simplest s-type Gaussians, rather than the higher-order Gaussian forms. Secondly Slater 3p, 4p, and 5p atomic orbitals which are written in the form of first order p Gaussian functions and same for 3d and 4d orbitals. These are expressed linearly in terms of second order Gaussian primitives. An expansion of atomic functions for given principal quantum numbers have a common set of Gaussian

exponents α is to be noted as additional feature. STO-3G minimal basis sets are used to calculate absolute energies of atoms and molecules in the form of properties such as energy differences, charge distributions, optimum geometries and electric dipole moments. With the exception of the total energy, the molecular properties calculated by using STO-3G basis sets, which gives reasonable results close to limiting values.

6-21G and **3-21G** split valence basis sets: [14,15]

The 6-21G and 3-21G basis sets are used to characterize the second and fourth row of periodic table with two basis functions used to describe each valence atomic orbital. These basis sets are used to represent outer shell orbitals (except for H) by two functions, one is contracted and the other is diffuse. In each case outer (diffuse) functions contain only one Gaussian while inner functions are made up of two Gaussians. Each inner-shell orbital (1s) for second row atoms are in the form of six Gaussian primitives in 6-21G basis set. Except for hydrogen, the 6-21G and 3-21G basis sets are employed to consider the changes during molecule formation without changes in the valence functions.

6-31G* and **6-31G**** basis sets:

These are the simplest polarization (*) basis sets originally proposed by Hariharan et.al.[16] for first-row atoms and later extended to second-row elements. 6-31G* basis set is the simplest form among these two polarization basis sets, 6-31G* and 6-31G**. For all second row atoms these basis sets use a single set of six second order functions (*), second order Gaussians to one s and five d orbitals, six Gaussian primitives for the core orbitals and a three/one split pair for each s and p valence orbital. Polarization of s orbitals on hydrogen atom is considered to be very important to describe its bonding in

many systems. 6-31G* and 6-31G** basis sets were similar in all functions except in describing the polarization due to hydrogen bonding. In addition to 6-31G*, 6-31G** use an extra set of p orbitals on H atoms to allow additional polarization.

6-311+G* and **6-311+G**** basis sets:

The 6-311+G* basis set was used to characterize first and second row elements by the addition of a single set of diffuse Gaussians (*) on the s and p-type functions. The 6311+G** basis set is comprised of six Gaussians for 1s orbitals of non H atoms, valence orbitals of all non H atoms, and a three way split valence for all H atoms. This set includes three Gaussians for the inner part and one Gaussian for the middle and outer parts. Several sets of data show that the effect of added diffuse functions (*) is more significant for negative charged species (O_2^-) than the corresponding neutral species (O_2).

2.5 DENSITY FUNCTIONAL THEORY

Density Functional Theory (DFT) is a quantum mechanical model used to determine the electronic structure of the ground state properties of molecules. In density functional theory, the energy is described as a "functional" of the density of a uniform electron gas ($E(\rho)$). In this theory, the electron system properties were determined using the functional to represent the spatial electron density. Some of the more common methods used in density functional theory are known as: BP86- developed by Becke and Perdew in 1986,[17] B3LYP- developed by Becke, Lee, Yang and Parr, B3LYP- a variation of BLYP in which a three - parameter functional developed by Axel Becke is used. The functional itself is a continuous electron gradient often originally shaped by participating atomic orbitals, but not dictated by them.

Hohenberg and Kohn (1964) expressed energy as a functional of the electron density, where the functional is independent of the system, and which applies only to the ground state. Kohn and Sham (1965) proposed various density equations for local functionals, where the density can be represented as a single determinant of orbitals, but the orbitals are not strictly in the form of Hartree-Fock.

The Thomas-Fermi Dirac model represents the energy as a function of the electron density including electron- electron repulsion J[ρ], and nuclear electron attraction V_{NE}.

$$V_{NE}[\rho] = \sum_A Z_A \int (\rho / r_A)\, d\tau \qquad [37]$$

$$J[\rho] = \int \rho(1)\, \rho(2)/r_{12})\, d\tau_1\, d\tau_2 \qquad [38]$$

For kinetic energy:

$$T[\rho] = c \int \rho^{5/3}\, d\tau \quad c = (3/10)\, (3\pi^2)^{2/3} \qquad [39]$$

For the exchange energy the Slater approximation expressed as

$$K[\rho] = c \int \rho^{4/3}\, d\tau \qquad c = (-9\alpha/8)\, (3\pi)^{1/3} \qquad \alpha=1 \qquad [40]$$

Density Functional theory is fundamentally a technique to solve the Schrodinger equation:

$$H\psi = E\psi \qquad [41]$$

The Hamiltonian operator H is a combination of both potential and kinetic energy operators, which account for electron interactions, nuclear-electron attraction, and coulombic repulsion of the nuclei and most importantly energy correlation of the electrons. DFT is considered accurate model in quantum chemistry for predicting the ground state energy of molecules.DFT defines an electron wave functional which considers electron interactions by means of their charge density. In DFT ψ denotes this functional, where various electronic properties are based on using this functional, (technically a function of the other functions), such as initial atomic orbitals, and which produces a final electron density distribution. The following various models were used for approximation of exchange correlation function.

a) Local density approximation Methods (LDA)

b) Non local extension to LDA

c) Hybrid Functional Methods.

Local density approximations are approximations used to estimate the exchange correlation energy functional for a homogenous electron gas. The assumptions are used to derive an expression for the kinetic energy of the electrons based on the electron density ρ(r). This kinetic energy and total energy functionals are expressed as follows, according to Thomas and Fermi.

$$T_{TF}(\rho) = (3/10)(3\pi^2)^{2/3} \int dr\, \rho^{5/3}(r) \qquad [42]$$

$$E_{TF}(\rho) = T_{TF}(\rho) - Z \int dr\, \rho(r)/(R-r) + \tfrac{1}{2} \int dr_1\, dr_2\, \rho(r_1)\, \rho(r_2)/(r_1 - r_2) \qquad [43]$$

They state that the energy is the sum of electronic kinetic energy (T), the electron nuclear attraction energy, and the Hartree correlation energy, where Z is the nuclear charge, and R is the position vector of the nucleus.

The first Hohenberg-Kohn theorem[18] notes: "The external potential v(r) is determined, within a trivial additive constant, by the electron density ρ(r)". The number of electrons determining the electron density, the wave function and all the ground state properties of the system are determined by this electron density. The proof of the theorem assumes the existence of two external potentials differing by a constant, and which lead to the same ground state density. This corresponds to the existence of two different Hamiltonians, with different wave functions, giving the same ground state electron density. The electron density determines all the ground state properties which include the total ground state energy E_{tot}, electron-electron repulsion energies W, energy of the electrons in the external potential U, and the ground state kinetic energy T. All of these are functionals of the electron density. Therefore the total energy is expressed as:

$$E^0\,(tot) = \; E_{tot}\,(\rho^0) = T\,(\rho^0) + U\,(\rho^0) + W\,(\rho^0) \qquad [44]$$

ρ^0 is the true ground state electron density of the system. The first Hohenberg-Kohn theorem thus describes the total energy functional, but it does not give the solution to the many body electron problems. The second Hohenberg-Kohn theorem states that for any given non- negative trial density, ρ(r) integrates to the total number of electrons, N, the true ground state energy E^0 (tot) is equal to or less than the computed E_{tot} using minimization procedures.

$$E^0\,(tot) \leq E_{tot}\,[\rho(r)] \qquad [45]$$

If T (ρ), U (ρ) and W (ρ) are known functionals, then there is a way to get solutions for the total energy by the minimization of E_{tot}. They also assumed that the external potential with the total number of electrons determines the Hamiltonian completely, and that these two quantities determine all the ground state properties of the system.

Kohn and Sham found a better approximation by treating the kinetic energy and unknown T(c), and W (ρ) functionals by introducing non-interacting orbitals of neutral density. Therefore the ground state density of the fully interacting system is exactly equal to the ground state density of non-interacting system; and they succeeded in showing the N-electron density decomposes into orbitals. These are known as Kohn-Sham orbitals (KS), and the expected value of the kinetic energy operator using these orbitals is the kinetic energy T_S (ρ) of non-interacting system.

When the Hohenberg-Kohn principle applies to the Kohn-Sham orbitals, this result in canonical Kohn-sham equation expressed by:

$$[-1/2(\partial^2/\partial\tau^2)_{i} + V_{eff}]\ \psi_i = \varepsilon_i\ \psi_i \qquad [46]$$

Where τ contain x, y, z coordinates and ε_i is the Kohn-Sham eigenvalue of electron i.

The effective potential is:

$$V_{eff}(r) = V_{ext}(r) + \int dr'\ \rho(r') / (r-r') + V_{xc}(r) \qquad [47]$$

Where $r^2 = x^2 + y^2 + z^2$. V_{ext} is the exchange -correlation and external potential to define the both exchange and correlation energy with respect to density.

$$V_{xc}(r) = \partial E_{xc}\ [\rho(r)] / \partial \rho(r) \quad [48]$$

These equations are non linear and similar to Hartree-Fock equations. Thus they are solved by a self consistent procedure. When the energy converges to a preset limiting value, the resultant density is expressed as:

$$\rho(r) = \sum_I \psi_i^*(r)\, \psi_i(r) \quad [49]$$

Kohn-Sham eigen value gives total ground state energy by using equivalent solution

$$E_{tot}(\rho) = T_s(\rho) + U(\rho) + H(\rho) + E_{xc}(\rho) \quad [50]$$

The "non local extension" to LDA is very important to maintain molecules in a heterogeneous electron gas. A hybrid functional requires Hartree-Fock treatment to give repulsion integrals.

2.6 MOLECULAR MECHANICS

Molecular mechanics are used in many preliminary computations to model the molecular systems and to study the molecules in biological system. Based on Hooke's law, the atoms act as point masses separated by a spring with a distinctive force constant K for each chemical bond between two adjacent atoms. Force is directly proportional to the displacement X_A (where $X = r - r_e$) and to the force constant of the spring.

$$F = -kx \quad [51]$$

Potential energy of spring is expressed as:

$$U = \frac{1}{2} kx^2 \quad [52]$$

In this method data output is evaluated according to parameterization of electronic and mechanical interactions of molecule, based on conventional bond lengths, angles and polarity. The potential energy of the molecule includes bending, stretching, and Vander Waals interactions (steric), torsional and bond dipole moments of the molecule. The atoms connected in this way form a frame work for subsequent electronic computation.

$$E = E_{stretch} + E_{bend} + E_{torsion} + E_{non\text{-}bonded\ interaction} \quad [53]$$

In general, molecular mechanics calculates the potential energy by force fields containing functional forms, parameters and atom types, where the atoms are preassigned to a specific atomic type based on its hybridization (e.g. sp^3, sp^2, sp, carbonyl, etc).The force field minimizes the stretched bond energies within the molecule, and forms a bond potential energy which is easily transferable between molecules (e.g. CH stretches in ethane is almost same as in butane).

MM2, MM3, AMBER, SYBYL, UFF, MMFF etc are a few of the molecular mechanical models, which are slightly different in their parameterization. Molecular mechanics calculate the energy associated with each conformation of the molecule. Molecular mechanics models are used for considering dynamics, vibrational analysis and potential energy surfaces. Force fields use a quadratic form to represent bond stretched potential energy.

$$E_{str} = \sum k_i (r\text{-}r_o)^2 \quad [54]$$

A Morse potential is more accurate for chemical bonds, but it is not used because it is asymmetric in the exponent, and therefore difficult to integrate.

$$E_{str} = \sum D_e [1\text{-}\exp(-\beta(r\text{-}r_0)]^2 \quad [55]$$

The bending terms are quadratic expressions as below, where $(\theta - \theta_0)$ are deflections from an equilibrium angle θ_0.

$$E_{bend} = \sum k_i (\theta - \theta_0)^2 \quad [56]$$

The non-bonded term includes electrostatic interactions, hydrogen bonded interactions and van der Waal forces.

$$E_{non\text{-}bond} = E_{vdW} + E_{es} + E_{Hbond} \quad [57]$$

Lennard-Jones potential expressed non-bonded terms (steric) in the form of

$$E_{vdW} = \sum 4\,\varepsilon_{ij}((\sigma_{ij} / r_{ij})^{12} - (\sigma_{ij} / r_{ij})^{6}) \quad [58]$$

Where σ (collision diameters) and ε (well depth) are tabulated, for pairs of atoms (ij) are obtained by the arithmetic and geometric means, respectively.

$$\sigma_{AB} = (\sigma_{AA} + \sigma_{BB})/2;\ \varepsilon_{AB} = (\varepsilon_{AA}\,\varepsilon_{BB})^{1/2} \quad [59]$$

For torsional energy the equation is expressed below.

$$E_{tors} = \sum V_i \cos[n(\theta - \theta_0)] \quad [60]$$

To fully represent a potential energy surface (e.g. vibrational and torsional motion) cross terms are required between bend, stretch and torsional motions. These are represented by the following additional terms.

$$E_{str\ -\ str} = \sum k_{ij} (r_{i\ -} r_{io\ )\ (}r_j - r_{j0}) \quad [61]$$

$$E_{str\ -\ bend} = \sum k_{ij} (r_{i\ -} r_{io}) (\theta_j - \theta_{j0}) \quad [62]$$

$$E_{bend\text{-}bend} = \sum k_{ij} (\theta_i - \theta_{i0}) (\theta_j - \theta_{j0}) \quad [63]$$

$$E_{bend\text{-}bend\ -tors} = \sum V_{ij} (\theta_i - \theta_{i0}) (\theta_j - \theta_{j0}) \cos [n (\theta_{ij} - \theta_{ij0})] \quad [64]$$

Steric energy refers to non-bonded interactions and is used to explain the different stable conformers of the same molecule. It also found that strainless molecules such as all trans hydrocarbons have no steric interactions. Force fields with identical structures and energies may contain different arbitrary terms, so it is ambiguous to factor the energy into individual parts due to bend torsion, stretching and non-bonded interactions.

The heat of formation (ΔH_f) of a molecule is computed here from the bond energies to form individual atoms and the atomization energy.

$$\Delta H_f = \Delta H_{atom} - \Delta H_{be} \quad [65]$$

Heats of formation of the atoms were calculated from the elements in their standards states at 298 K and 1 bar and then compared with experimental data.

2.7 GEOMETRY OPTIMIZATION[19]

In molecular modeling we are generally interested in minimum points on potential energy surfaces. This is because any movement away from a minimum gives a configuration with a higher potential energy and less stability. Energy surfaces may contain a large number of minima. The “global” energy minimum is the minimum with the very lowest energy. A minimization algorithm is used to find the geometries of the system that correspond to minimum points on the energy surface. Most minimization

algorithms can go “downhill” on the energy surface and they can locate the minimum that is nearest to the starting point.

In molecular modeling two different types of algorithms are commonly used to solve the general equation for minimization. First-order minimization algorithms are the methods of steepest descents and conjugate gradients. Conjugate gradient and quasi-Newton methods have good convergence with analytical and numerical gradients. The Newton-Raphson method is the simplest second-order method used for the second derivatives and also for the first derivatives (i.e. the gradients) to locate the minimum. Second derivatives provide information about the curvature of the function, and are needed to find normal vibrational mode frequencies.

When optimization fails there are various steps that we need to follow. If the output shows the program exceeded a preset number of cycles, then we have to check for strongly coupled coordinates or very flexible coordinates. The number of cycles in the options menu may need to be increased when the calculation is set up. “Geometry cycle=N” is the Spartan command in our work. The highest point on the pathway between two minima is known as a “saddle point”, where the atoms are being arranged in a transition state structure. The following general flow diagram represents the steps of geometry optimization for energy minima (ground states).

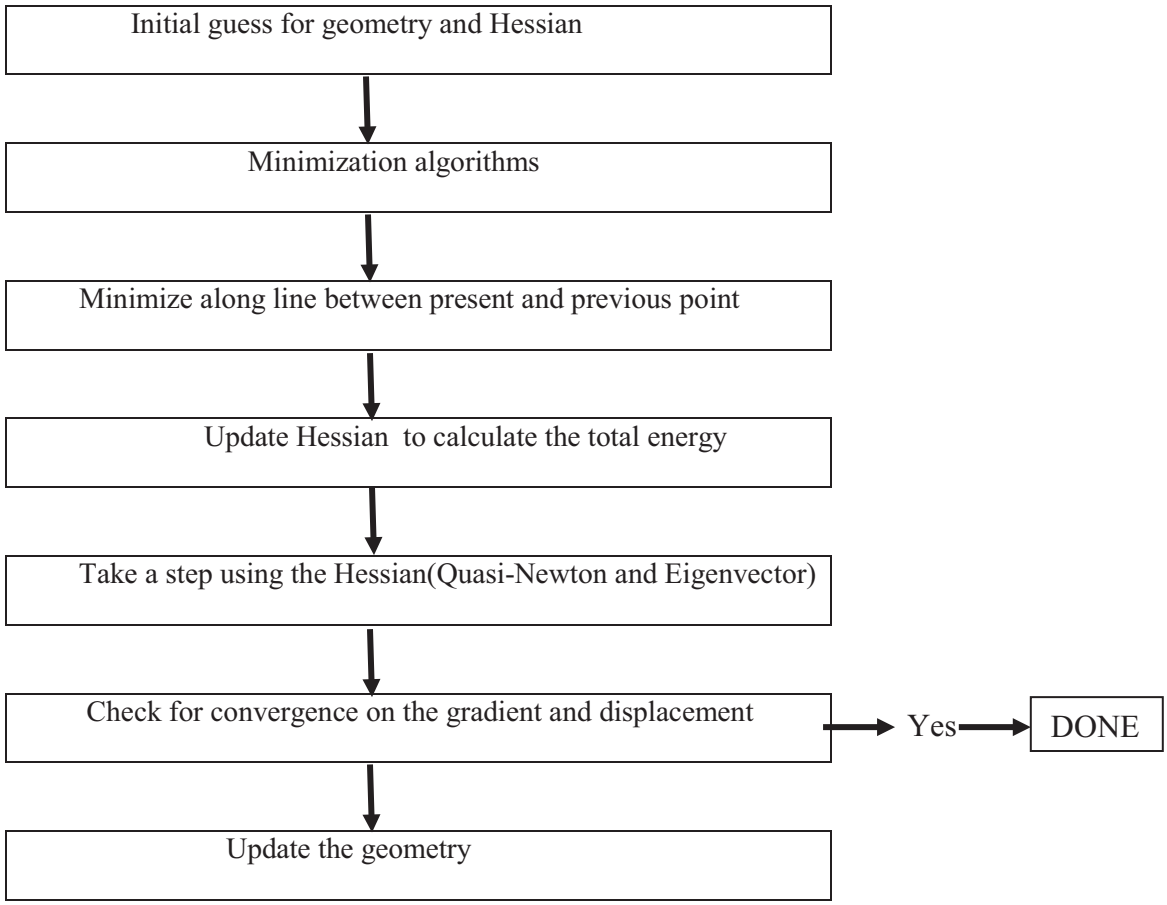

The choice of minimization algorithm depends up on various factors such as storage, computational efforts and the relative speeds of different parts to perform calculations and availability of analytical derivatives. Thus, any method that requires the Hessian matrix ($\partial^2 E/ \partial e_i^2$) to be stored is computationally demanding for systems that contain hundreds of atoms. The Hessian matrix of second derivatives must be definite in minimization to give positive eigenvalues (except for transition states). Quantum mechanical calculations are restricted to systems with relatively small number of atoms, so storing the Hessian matrix is usually not a problem. As the minimum energy calculation is often the most time-consuming part of any problem, it is desirable that the minimization method take as few steps possible to reach the minimum. For transition

states the Hessian is also necessary, but one normal mode is imaginary, corresponding to the energy maximum, and all other coordinates are energy minimized.

2.8 TRANSITION STATES

Empirical approaches use force field models for studying chemical reactions, which may also be used to compute activation energies of possible transition states. The force field model is usually developed by extending an existing force-field to enable the structures and relative energies of a transition structure to be determined. The force field is parameterized to produce an optimum geometry and relative energy, which is a maximum along the reaction coordinate but a minimum along all other coordinates. To simulate chemical reactions in solution a combination of quantum mechanics and molecular mechanics is used. The reacting parts of the system are treated quantum mechanically, and the remainder is modeled using a less computationally demanding force field. The total energy E_{TOT} for the system can be written as

$$E_{TOT} = E_{QM} + E_{MM} + E_{QM/MM.} \quad [66]$$

E_{QM} is the energy of those parts of the system treated by quantum mechanics, and E_{MM} is the energy of the molecular mechanical parts of the system. $E_{QM}/_{MM}$ is entirely due to non-bonded interactions between the molecular mechanical and quantum mechanical atoms of the systems. In some cases the quantum mechanical and molecular mechanical regions are in the same molecule, which contains bonds between atoms from each region.

We are not only interested in the thermodynamics of a process (the relative energy of the initial and final species that define the total thermodynamic driving force),

but also in the transition state geometry and activation energy. Thermodynamic data can be computed knowing the minimum points on energy surfaces. We also use computational methods to find an energy maximum along one reaction coordinate, which is a normal vibration with an imaginary frequency. When we are at a successfully optimized transition state, we still need to know the energy variation that occurs during the reaction coordinate change in geometry. For this we input an initial estimate of the transition state geometry, and ensure that the coordinates dominating the decomposition vector are not strongly coupled to the remaining vibrational coordinates. The program then examines the initial Hessian for a negative eigenvalue, which refers to the decomposition motion.

Our work used Spartan 2004* for building and locating the transition states. To calculate transition states software helps in providing both an extensive and extendable states to match the possible entries in the library with the reaction. If the reaction is unknown to the library (as for the present case using Cu^{2+}), a fall back technique is used in the software which is similar to the "linear synchronous transit method". The synchronous transit guides the transition state search between the average geometries of reactant and product, so that there is optimization in redundant internal coordinates only one of which results in decomposition. Two alternative steps are involved:

1) QST2: The input reactant-like structure is guided to a product-like structure by directed electron flow as bonds are broken and formed. An initial estimate of the transition state is approximated by a linear interpolation of redundant internal coordinates.

2) QST3: Estimate the transition state by the input of reactant and product structures with no intermediate.

The first few steps find maxima along a path and the remaining steps use regular transition state optimization methods. If the transition state vector deviates from the optimal path it automatically selects an improved vector. Depending on the level of theory, the current dismutation reaction required 60 to 120 steps to reach the optimization without copper ion and 150 to 180 steps with copper ion.

2.9 THERMODYNAMICS[19]

A wide variety of thermodynamic properties can be calculated from computer simulations, and a comparison of experimental and computed values is an important way to evaluate the accuracy of the simulation and thus the sufficiency of the underlying theoretical model. Simulations also enable predictions to be made where there is no experimental data, or for which experimental data is difficult to obtain. They also provide structural information about the conformal changes in molecules, and the thermal distributions of molecules among energy states available in a system. Unfortunately, the free energy is difficult to obtain in the systems containing liquids or flexible macromolecules that have many minimum energy configurations separated by low-energy barriers.

According to the classical equation below, the equilibrium constant for a chemical reaction is a thermodynamic property of the reactants and products and is a function of the standard Gibbs free energy, ΔG^0.

$$\Delta G^0 = -RT\ln K_e \qquad [67]$$

T denotes the absolute temperature, R is the gas constant in J/mol k and K_e is the equilibrium constant. In general, $\Delta G > 0$ refers to a nonspontaneous reaction; which tends to be spontaneous in the opposite direction.

$\Delta G = 0$ refers to an equilibrium state of the reaction;

$\Delta G < 0$ refers to a reaction which tends to be spontaneous reaction;

ΔG^0 is related to standard enthalpy and entropy of the reaction by the following equation. The superscript (^{0}) refers to the standard conditions at 298K and 1 bar pressure.

$$\Delta G^0 = \Delta H^0 - T\Delta S^0 \qquad [68]$$

Our calculations give ΔH_f^0 (or E^0-H^0 for HF and DF methods) and S^0 for individual compounds, either indirectly or directly from which we calculate ΔH_{rxn}, ΔS_{rxn} and ΔG_{rxn} in the usual manner.

The rate constant of a reaction is a kinetic property and it may be related to the activation energy E_a by the Arrhenius equation:

$$\ln k_1 = \ln A - E_a/RT \qquad [69]$$

k_1 is the rate constant and A is a frequency factor. The alternative Eyring equation gives a relation which contains the rate constant and the approximate equilibrium constant between the reactants and transition state:

$$k_1 = (kT/h)K^{\dagger} \qquad [70]$$

k is Boltzmann constant, h is Planck constant and $K^{\dagger}$ is the equilibrium constant. The superscript (†) refers to the transition state. The activation free energy is related to the

enthalpy of activation and entropy of activation by the analogous thermodynamic equation

$$\Delta G^{\dagger} = \Delta H^{\dagger} - T\,\Delta S^{\dagger} \qquad [71]$$

The Arrhenius activation energy E_a is related to the Eyring enthalpy of activation $\Delta H^{\dagger}$ by the given equation below, where two product molecules result from one transition state.

$$E_a = \Delta H^{\dagger} + 2RT \qquad [72]$$

2.10 EFFECT OF SOLVATION

Most computer models are based on individual gas phase molecules or ions in a vacuum, so that reactions in solution may not be directly comparable due to solvent effects. These are nearly impossible to compute in a specific way, but they may be approximated in molecular mechanics calculations using a parameter for a dielectric continuum related to the solvent dielectric constant. Generally when considering changes in entropy and geometry these effects are small, but energy effects (enthalpy) may be significant in processes involving changes in polarity, possibly ±10% of the bond energies involved. In our chemical reactions containing charge dispersed initial and transition states, polar solvent stabilization will affect similarly both states. Since the neutral products O_2 and H_2O_2 are not as highly polarized, but they would not be stabilized as much as the ionic reactants, so the solvated exothermicities are expected to be less than the unsolvated ones. In comparing reaction mechanisms these effects would likely cancel out since in all cases the same ions are converted to the same neutral molecules using the same Cu^{2+}/ Cu^{+} catalysts.

3. RESULTS AND DISCUSSION

This investigation is done using three types of computational theory to determine the reactive thermodynamic properties (ΔH, ΔG and ΔS). Hartree-Fock (HF), semi-empirical (SE) and density functional (DF-B3LYP). They were used with different basis sets selected to be the most efficient and precise for our computer platforms. We finally choose the 6-31G* as a practical compromise between efficiency and accuracy, for the most complex transition state-the largest calculation. Superoxide dismutase catalyses the overall dismutation reaction of the superoxide radical anion to molecular oxygen and hydrogen peroxide.

$$2O_2^- + H_3O^+ + HArg^+ \longrightarrow O_2 + H_2O_2 + H_2O + Arg \qquad [73]$$

Our choice of H^+donors H_3O^+ and $HArg^+$ is based on the suggestion of Osman and Bach[9,10] and H_3O^+ are often chosen as convenient source of H^+ in enzymatic reactions. For simplicity in notation, the conventional $[Cu(NH_3)_4(H_2O)_2]^{2+}$ symbols for the coordinated Cu^{2+}/ Cu^+ ions are dropped in the mechanisms listed below. $^{\cdot}OOH$ is formed and destroyed between the two steps.

Mechanism 1:

Step 1: $Cu(NH_3)_4(H_2O)_2^{2+} + O_2^- \rightarrow Cu(NH_3)_3(H_2O)^+ + O_2 + NH_3 + H_2O$

Step 2: $Cu(NH_3)_3(H_2O)^+ + O_2^- + H_3O^+ + HArg^+ + NH_3 \rightarrow Cu(NH_3)_4(H_2O)_2^{2+} + H_2O_2 +$ Arg

Mechanism 2:

Step 1: $Cu(NH_3)_4(H_2O)_2^{2+} + O_2^- \rightarrow Cu(NH_3)_3(O_2)^+ + 2H_2O + NH_3$

Step 2: $Cu(NH_3)_3(O_2)^+ + O_2^- \rightarrow O_2 + Cu(NH_3)_3(O_2)$

Step 3: $Cu(NH_3)_3(O_2) + NH_3 + H_2O + H_3O^+ + HArg^+ \rightarrow Cu(NH_3)_4(H_2O)_2^{2+} + H_2O_2 +$ Arg

Mechanism 3:

Step 1: $Cu(NH_3)_4(H_2O)_2^{2+} + O_2^- \rightarrow Cu(NH_3)_3(O_2)^+ + 2H_2O + NH_3$

Step 2: $Cu(NH_3)_3(O_2)^+ + O_2^- + H_3O^+ \rightarrow O_2 + Cu(NH_3)_3(OOH)^+ + H_2O$

Step 3: $Cu(NH_3)_3(OOH)^+ + HArg^+ + 2H_2O + NH_3 \rightarrow Cu(NH_3)_4(H_2O)_2^{2+} + H_2O_2 + Arg$

Mechanism 4:

Step 1: $Cu(NH_3)_4(H_2O)_2^{2+} + O_2^- \rightarrow Cu(NH_3)_3(H_2O)^+ + O_2 + NH_3 + H_2O$

Step 2: $Cu(NH_3)_3(H_2O)^+ + O_2^- + H_3O^+ \rightarrow Cu(NH_3)_3(OOH)^+ + 2H_2O$

Step 3: $Cu(NH_3)_3(OOH)^+ + HArg^+ + 2H_2O + NH_3 \rightarrow Cu(NH_3)_4(H_2O)_2^{2+} + H_2O_2 + Arg$

Mechanisms 1 and 2, the most commonly mentioned in the literature, involve either a simultaneous collection of three reactants in one step (Mechanism 1, step 2; M1S2), which is statistically unlikely, or the postulation of a neutral copper complex with molecular O_2 (M2S2),which is also unlikely.

Mechanisms 3 and 4 are suggested to include the more likely stepwise reduction of superoxide to peroxy radical ($O_2^- + H^+ \rightarrow HO_2^{\cdot}$), the only difference being how the

peroxy radical forms via the O_2 complexed to Cu^+ (M3) or the reduced second O_2^- displacing H_2O from the Cu^+ shell (M4).

Within these 4 mechanisms it has been suggested that a bond ligating Cu^{2+} to His 61 breaks forming a very basic imidazolate group (I), which later receives a H^+ from H_3O^+, leaving the Cu^{2+} ligated by one less Cu-N coordinate bond. We model this process when Cu^{2+} is reduced to Cu^+, and the octahedral Cu^{2+} complex converts to tetrahedral Cu^+ complex and releases one NH_3 molecule. The symbols Cu^{2+} and Cu^+ refer to these complex ions and the NH_3 molecules mimic the approximately co-planar histidine residue in the active site ligating the copper ion. One of the NH_3 ligands separate in each first step and reattaches later in the final step of each mechanism. We also found the substituting imidazole rings (as in histidine) the NH_3 molecules made no significant difference in the overall thermodynamics.

On a technical note, the higher level treatments and Hartree-Fock gave their energies for each substance in atomic units (au), not the more common calories or joules. One au is equal to 627.5 kcal, or 2625kJ/au since the standard states for the higher level calculations (HF and DF) were separated nuclei and electrons, no direct energy comparison could be made between experiment and theory (except for SE) from compound to compound. However, when the energy differences for the reaction were computed in au, the related values in joules or calories could easily be made using the conversion factor above.

3.1 THERMODYNAMICS

The heats of formation and entropies including transitional, vibrational and rotational degrees of freedom were calculated for the stable reactants and products by the standard statistical thermodynamic methods incorporated in the Spartan program. The well known equation connecting the Gibbs energy, ΔG, for the chemical reactions are used for our evaluation of mechanistic alternatives. Thus, $\Delta G = - RTlnK_e$ and $\Delta G = \Delta H - T\Delta S$ are the linkages between ΔH and ΔS, the enthalpies and entropies of our reactions, and their thermodynamic tendency to occur. From the computed data for each substance we calculated ΔH_{rxn}, ΔS_{rxn} and ΔG_{rxn} at different levels like semi-empirical (SE, PM3), Hartree-Fock (HF, 6-31G*, 6-31G**) and density functional (DF, B3LYP at6-31G*.6-31G**) for a given reaction.

$$\Delta H_{rxn} = \sum_p . \Delta H^0_{f,p} - \sum_p . \Delta H^0_{f,r}$$

Where p = products and r = reactants, ΔS_{rxn} is calculated in the same manner.

3.2 METAL ION EFFECT

It is known that Cu^{2+} is directly involved in the catalytic activity[20], where as Zn^{2+} has a structural and stabilizing role in the active site. Copper also plays an important entropic role in steering protons (H_3O^+ or $HArg^+$) to the superoxide at the active site, to form molecular oxygen and hydrogen peroxide. Secondly the Cu^{2+}/Cu^+ ions act as redox centers which lower the potential energy barriers to electron transport, and hence lower the E_a values. Rehybridization of the Cu^{2+} orbitals (sp^3d^2-octahedral) to Cu^+ orbitals (sp^3-tetrahedral) also has an energetic cost which is paid for by the exoergicity of the overall reaction.

If one compares a "concerted" transition state in a square planar form ($2O_2^-$ + H_3O^+ + $HArg^+$) both with and without a central Cu^{2+}, it is clear that Cu^{2+} lowers the activation energy presumably by playing an electron relay role. Table 1 and 2 compare the number of optimization steps required for the calculation of the "concerted" dismutation reaction both with and without copper using only the four elementary reactants and products organized in a square planar geometry, with or without a central uncomplexed Cu^{2+}. It is clear that the higher the level of theory, the more cycles are required for optimization to be completed, and that Cu^{2+} plays a redox mediation role.

3.2.1 Effect of Cu^{2+} on basic reaction

Table 1. Number of optimization steps required for dismutation reaction without copper ion

Level of Theory (Basis sets)	Number of optimization steps without copper	Activation Energy without copper(kcal)
PM3	60	44.07
DF- 6-31G*	130	35.6
DF- 6-31G**	130	27.25
HF - 6-31G*	90	30.52
HF - 6-31G**	95	35.52

Table 2. Number of optimization steps required for the dismutation reaction with copper ion

Level of Theory (Basis sets)	Number of optimization steps with copper	Activation Energy with copper (kcal)
PM3	140	15.5
DF- 6-31G*	175	9.2
DF- 6-31G**	175	9.5
HF - 6-31G*	175	5.2
HF - 6-31G**	175	5.2

3.2.2 Computation times of dismutation reaction

The following twenty tables summarize: (a) the times required to optimize the thermodynamic parameters for the elementary reaction; (b) the C-N distances in the crystal structure of the active site compared with the calculated values; (c) the thermodynamic parameters and transition state energies for all the steps of the four suggested mechanisms.

Table 3. Computation times of the dismutation reaction at different levels

Theoretical Methods	Computation time taken for reactants from ground state to transition state without copper (minutes)	Computation time taken for reactants from ground state to transition state with copper (minutes)
PM3	42	60
DF(6-31G*)	380	2020
DF(6-31G)**	426	2120
HF (6-31G*)	245	2412
HF (6-31G)**	220	2115

3.2.3 Active site model

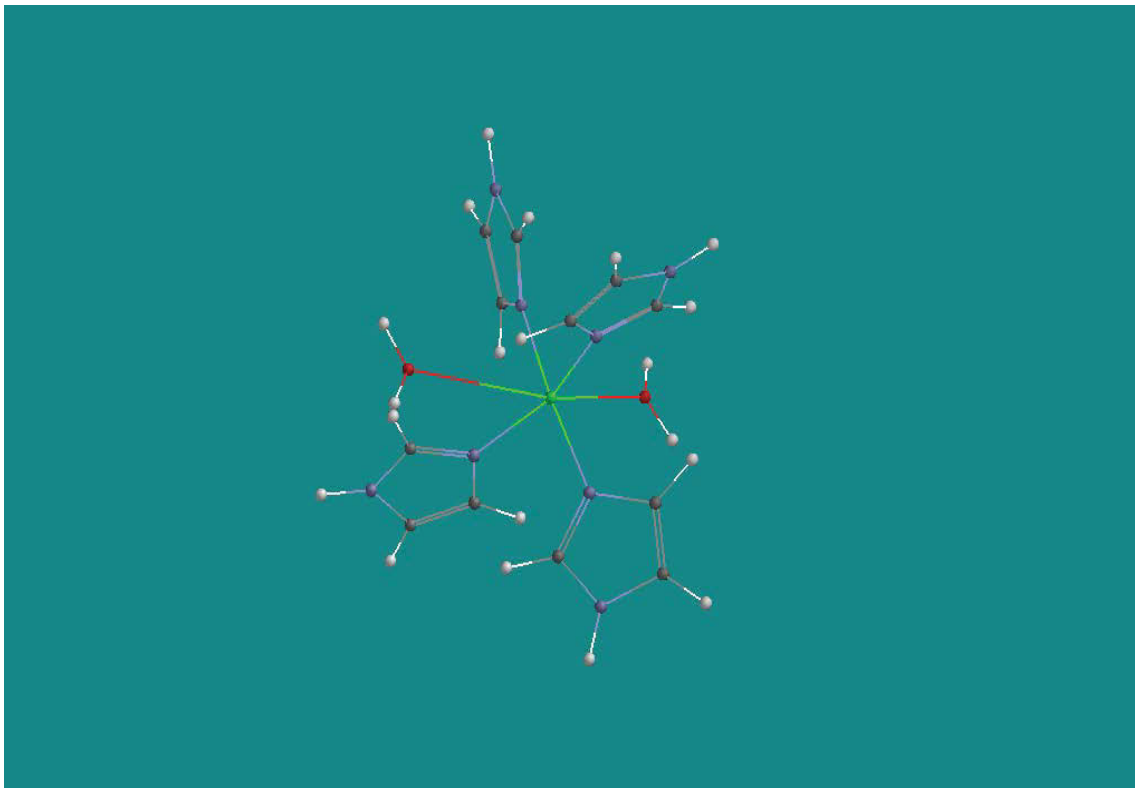

Figure 2 Optimized structure of simplified active site [Cu (Imidazole)4$(H_2O)_2$]$^{2+}$

The computed bond distances in the modeled "imidazole" catalytic center, in the optimized structure are studied. Pseudo potential approach, known as PAW (Car-Parinello Projector Augmented Wave method) this process is computationally demanding for transition metal atoms and uses of simple plane-wave basis set. Carolini *et al*. calculated these bond distances of the four imidazole molecules in a simplified active site of optimized structure in 1995 in which the calculations are performed by a using IBM/RS6000 530,540 and 550 work stations[7]. The results shows good comparison between bond distances of SPARTAN, PAW, and the experimental crystal structure, showing that the DF theory with 6-31G* initial basis functions are adequate to give

realistic geometries. Green bonds connect Cu^{2+} with four imidazole and two water molecules, coordinated by lone pair electrons on the Levis base atom.

3.2.4 Bond distances in imidazole molecule in the optimized structure

Table 4. Comparison between bond distances in imidazole molecule in the optimized structure by PAW, crystal structure, and optimized structure by B3LYP/6-31G* in Spartan 2004[7]

	SPARTAN 2004 (A^0)	PAW (A^0)	CRYSTAL STRUCTURE (A^0)
N(1)-C(2)	1.378	1.374	1.358
N(1)-C(5)	1.396	1.384	1.381
C(2)-N(3)	1.338	1.329	1.333
C(5)-N(3)	1.396	1.384	1.389
C(4)-C(5)	1.042	1.378	1.378
N(1)-H(1)	1.108	1.036	1.053
C(2)-H(2)	1.106	1.103	1.087
C(4)-H(4)	1.104	1.102	1.086

It was earlier mentioned that the energetics of selected catalytic reactions (M1S1, M2S2) were unaffected whether using $[Cu\ (NH_3)_4\ (H_2O)_2]^{2+}$ or $[\ Cu\ (Imid)_4\ (H_2O)2]^{2+}$. Thus the modeling simplification of using NH_3 in place of the active site histidine (imidazole) is justified.

3.2.5 Heats of formation for simplest dismutation reaction components

Table 5. Heats of formation for simplest dismutation reaction components (kcal/au)

Theoretical Method(basis sets)	O_2^-	H_3O^+	O_2	H_2O_2	H_2O
SE(PM3) (kcal/mol)	-13.275	159.072	18.385	-40.789	-53.427
DF(6-31G*) (au/mol)	-150.289	-76.891	-151.545	-151.542	-76.418
DF(6-31G) (au/mol)**	-150.289	-76.688	-151.551	-151.586	-76.0423
HF (6-31G*) (au/mol)	-149.563	-75.892	-150.786	-150.881	-75.585
HF (6-31G) (au/mol)**	-149.564	-75.895	-150.796	-150.776	--75.896
Experimental Values (kcal/mol)	-11.620	138.900	0.00	-32.53	-57.801

There are 625.7 kcal/au or 2,625 kJ/au. For DF and HF methods, $\Delta H_f = E^0 - H^0$, where E^0 is the electronic energy and H^0 is the enthalpy of heating to 298 K.

The following table summarizes the fundamental thermodynamic quantities for the components of the overall reaction using $2H_3O^+$. Note only the semi-empirical result predicts the experimental quantities with in a wide margin of error.

3.2.6 Absolute entropies of the simplest dismutation reaction components

Table 6. Absolute entropies of the simplest dismutation reaction components (cal/Kmol)

Theoretical Method(Basis sets)	O_2^-	H_3O^+	O_2	H_2O_2	H_2O
SE(PM3)	46.96	46.389	46.675	54.785	44.951
DF(6-31G*)	47.257	46.183	46.82	53.355	45.25
DF(6-31G)**	47.252	46.185	46.80	53.325	45.95
HF (6-31G*)	47.08	46.125	46.65	54.002	44.68
HF (6-31G)**	47.09	46.129	460.82	54.025	44.856
Experimental Values	50.09	45.95	49.03	55.69	45.13

The comparison of theoretical with experimental values shows reasonable agreement within (5-10%) independent of the level of theory or basis set for these simple molecules using $2H_3O^+$.

3.2.7 ΔH_{rxn}, ΔS_{rxn} and ΔG_{rxn} of our dismutation reaction at different methods and basis sets

Table 7 shows computed values of ΔH_{rxn}, ΔS_{rxn} and ΔG_{rxn} with different methods and basis sets for following reaction. Note that the types of theory predict ΔS_{rxn} very consistently and in close agreement with the semi-empirical result. Also ΔH and ΔG are nearly the same values showing that ΔH_{rxn} also is an accurate measure of reaction tendency here.

Table 7. ΔH_{rxn}, ΔS_{rxn} and ΔG_{rxn} of our dismutation reaction at different methods and basis sets (kcal/Kmol)

Theoretical Methods (Basis sets)	ΔH_{rxn}	ΔS_{rxn}	ΔG_{rxn}
SE(PM3)	-395.029	0.005	-397.56
DF(6-31G*)	-395.19	0.003	-396.28
DF(6-31G)**	-395.24	0.003	-396.29
HF (6-31G*)	-380.15	0.004	-383.15
HF (6-31G)**	-380.88	0.004	-383.45
Experimental	-402.75	0.003	-403.56s

The standard temperature is 298 K. The fact that all levels of theory show good agreement for these reaction parameters implies that any errors for a particular compound subtract out.

3.2.8 Computed thermodynamic properties for given mechanism

Table 8 shows computed values of ΔH_{rxn}, ΔS_{rxn} and ΔG_{rxn} with different methods and basis sets for given O_2^-, H_3O^+ and $HArg^+$ overall reaction, which applies to all four mechanisms.

Overall reaction: $2O_2^- + H_3O^+ + HArg^+ \rightarrow O_2 + H_2O_2 + H_2O + Arg$

Table 8. Computed Thermodynamic Properties for given mechanism

Theoretical methods (Basis sets)	ΔH_{rxn} (kJ/mol)	ΔS_{rxn} (kJ/mol)	ΔG_{rxn} (kJ/mol k)
SE(PM3)	-809.2	0.004	-810.52
DF(6-31G*)	-637.9	0.002	-638.52
DF(6-31G)**	-637.85	0.002	-638.95
HF (6-31G*)	-639.52	0.001	-640.52
HF (6-31G)**	-639.52	0.001	-640.59

It is worth commenting that the use of $HArg^+$ instead of H_3O^+ as the source of the second proton makes the computed thermodynamic driving force about 60% greater (-650kJ vs. -400 kJ for the $2H_3O^+$ reaction). Since all four mechanisms work with these same reactants and products, all four here the same driving force.

3.2.9 Heats of formation of dismutation reaction catalytic components

Table 9 Shows computed values of heats of formation of the given catalytic components of SOD mechanisms. The following table shows the calculated heats of formation, entropy (sum of rotational, transitional and vibrational) with the different types of theory and basis sets.

Table 9. Heats of formation of the dismutation reaction catalytic components (SE, kcal and (DF, HF au)

Theoretical Methods (Basis sets)	$Cu(NH_3)_4(H_2O)_2^{2+}$	$Cu(NH_3)_3H_2O^+$	$Cu(NH_3)_3OOH$	$Cu(NH_3)_3O_2$
SE(PM3) (kcal/mol)	50.595	-116.114	-27.163	-32.759
DF(6-31G*) (au/mol)	-2018.935	-1886.243	-1960.776	-1960.123
DF(6-31G) (au/mol)**	-2018.956	-1886.257	-1960.254	-1960.254
HF(6-31G*) (au/mol)	-2015.157	-1883.143	-1957.467	-1956.658
HF(6-31G) (au/mol)**	-2015.235	-1883.157	-1957.568	-1956.648

Note here the consistency between both the HF and DF methods using the closely related basis sets. The mechanistic details for the generally accepted (Osman and Bash[9,10])two step and three step mechanisms we modeled using the catalytic species of Cu^{2+} and

Cu^{+} ligated to the active site by four imidazole ring systems as represented by NH_3 molecules. We now consider the thermodynamics of the various mechanistic steps.

3.2.10 Computed thermodynamic properties for all four mechanisms

Table 10 shows computed values of ΔH_{rxn}, ΔS_{rxn} and ΔG_{rxn} with different methods and basis sets for following reaction. Note that the different types of theory predict ΔS_{rxn} very consistently and in close agreement with the semi-empirical result.

Mechanism 1 (step 1):

$$Cu(NH_3)_4(H_2O)_2^{2+} + O_2^{-} \rightarrow Cu(NH_3)_3(H_2O)^{+} + O_2 + NH_3 + H_2O$$

Table 10. Computed Thermodynamic Properties for mechanism1 step 1 (M1S1)

Theoretical Methods (Basis sets)	ΔH_{rxn} (kJ/mol)	ΔS_{rxn} (kJ/mol)	ΔG_{rxn} (kJ/mol k)
SE(PM3)	48.59	+0.348	-55.71
DF(6-31G*)	420.58	+0.350	316.22
DF(6-31G)**	420.87	+0.350	316.22
HF (6-31G*)	425.34	+0.350	321.04
HF (6-31G)**	425.37	+0.350	321.08

It is worth noting that the semi-empirical calculation gives the only spontaneous (-ΔG_{rxn}) tendency due to the increased randomness in the entropic term. The major

difference is in the endothermicity of the semi-empirical ΔH_{rxn} being of the order of 10% of that for the DF and HF methods. The apparent unlikelihood of this step is compensated for by the –ΔH's and –ΔG's in subsequent steps.

Table 11 shows computed values of ΔH_{rxn}, ΔS_{rxn} and ΔG_{rxn} with different methods and basis sets f0r following reaction. Note that the types of theory predict ΔS_{rxn} very consistently and in close agreement with the semi-empirical result.

Mechanism 1 (step 2):

$$Cu(NH_3)_3(H_2O)^+ + O_2^- + H_3O^+ + HArg^+ + NH_3 \rightarrow Cu(NH_3)_4(H_2O)_2^{2+} + H_2O_2 + Arg$$

Table 11. Computed Thermodynamic Properties for mechanism1 step 2 (M1S2)

Theoretical Methods (Basis sets)	ΔH_{rxn} (kJ/mol)	ΔS_{rxn} (kJ/mol)	ΔG_{rxn} (kJ/mol k)
SE(PM3)	-856.52	-0.344	-754.01
DF(6-31G*)	-1060.52	-0.348	-956.81
DF(6-31G)**	-1060.53	-0.348	-956.81
HF (6-31G*)	-1065.53	-0.349	s-961.53
HF (6-31G)**	-1065.58	-0.348	-961.54

Table 12 shows computed values of ΔH_{rxn}, ΔS_{rxn} and ΔG_{rxn} with different methods and basis sets for following reaction. Note that the different types of theory predict ΔS_{rxn} very consistently and in close agreement with the semi-empirical result.

Mechanism 2 (step 1):

$$Cu(NH_3)_4(H_2O)_2^{2+} + O_2^- \rightarrow Cu(NH_3)_3(O_2)^+ + 2H_2O + NH_3$$

Table 12. Computed Thermodynamic Properties for mechanism 2 step 1 (M2S1)

Theoretical Methods (Basis sets)	ΔH_{rxn} (kJ/mol)	ΔS_{rxn} (kJ/mol)	ΔG_{rxn} (kJ/mol k)
SE(PM3)	97.5	+0.350	-6.1
DF(6-31G*)	473.95	+0.350	369.65
DF(6-31G)**	473.95	+0.350	369.65
HF (6-31G*)	473.91	+0.350s	369.64
HF (6-31G)**	473.91	+0.350	369.68

Note here the greater endothermicity and +ΔG for this step compared to step 1 of the previous mechanism (M1S1) with the higher theoretical methods.

Table 13 shows computed values of ΔH_{rxn}, ΔS_{rxn} and ΔG_{rxn} with different methods and basis sets for following reaction.

Mechanism 2 (step 2):

$$Cu\ (NH_3)_3\ (O_2)^+ + O_2^- \rightarrow O_2 + Cu\ (NH_3)_3\ (O_2)$$

Table 13. Computed Thermodynamic Properties for mechanism 2 step 2 (M2S2)

Theoretical Methods (Basis sets)	ΔH_{rxn} (kJ/mol)	ΔS_{rxn} (kJ/mol)	ΔG_{rxn} (kJ/mol k)
SE(PM3)	132.5	-0.001	132.7
DF(6-31G*)	-1190.50	-0.104	-1160.5
DF(6-31G)**	-1190.50	-0.104	-1160.2
HF (6-31G*)	-1190.52	-0.104	-1159.5
HF (6-31G)**	-1190.53	-0.104	-1159.5

Table 14 shows computed values of ΔH_{rxn}, ΔS_{rxn} and ΔG_{rxn} with different methods and basis sets for following reaction. Note that the different types of theory predict ΔS_{rxn} very consistently and in close agreement with the semi-empirical result.

Mechanism 2 (step 3):

$$Cu(NH_3)_3(O_2) + NH_3 + H_2O + H_3O^+ + HArg^+ \rightarrow Cu(NH_3)_4(H_2O)_2^{2+} + H_2O_2 + Arg$$

Table 14. Computed Thermodynamic Properties for mechanism 2 step 3 (M2S3)

Theoretical Methods (Basis sets)	ΔH_{rxn} (kJ/mol)	ΔS_{rxn} (kJ/mol)	ΔG_{rxn} (kJ/mol k)
SE(PM3)	-1018.52	-0.244	-948.2
DF(6-31G*)	78.65	-0.244	151.362
DF(6-31G)**	78.71	-0.244	151.351
HF (6-31G*)	78.72	-0.245	151.721
HF (6-31G)**	70.85	-0.245	151.732

Table 15 shows computed values of ΔH_{rxn}, ΔS_{rxn} and ΔG_{rxn} with different methods and basis sets for following reaction. Note that the different types of theory predict ΔS_{rxn} very consistently and in close agreement with the semi-empirical result.

Mechanism 3 Step 1:

$$Cu(NH_3)_4(H_2O)_2^{2+} + O_2^- \rightarrow Cu(NH_3)_3(O_2)^+ + 2H_2O + NH_3$$

Table 15. Computed Thermodynamic Properties for mechanism 3 step 1 (M3S1)

Theoretical Methods (Basis sets)	ΔH_{rxn} (kJ/mol)	ΔS_{rxn} (kJ/mol)	ΔG_{rxn} (kJ/mol k)
SE(PM3)	97.5	+0.350	-6.1
DF(6-31G*)	473.95	+0.350	369.65
DF(6-31G)**	473.95	+0.350	369.65
HF (6-31G*)	473.91	+0.350	369.61
HF (6-31G)**	473.91	+0.350	369.61

Table 16 shows computed values of ΔH_{rxn}, ΔS_{rxn} and ΔG_{rxn} with different types and basis sets for the following reaction. Note that the different types of theory predict ΔS_{rxn} very consistently and in close agreement with the semi-empirical result.

Mechanism 3 (step 2):

$$Cu(NH_3)_3(O_2)^+ + O_2^- + H_3O^+ \rightarrow O_2 + Cu(NH_3)_3(OOH)^+ + H_2O$$

Table 16. Computed Thermodynamic Properties for mechanism 3 step 2 (M3S2)

Theoretical Methods (Basis sets)	ΔH_{rxn} (kJ/mol)	ΔS_{rxn} (kJ/mol)	ΔG_{rxn} (kJ/mol k)
SE(PM3)	-750.2	-0.104	-720.2
DF(6-31G*)	-1087.5	-0.104	-1056.5
DF(6-31G)**	-1087.5	-0.104	-1056.5
HF (6-31G*)	-1087.3	-0.104	-1056.3
HF (6-31G)**	-1085.3	-0.104	-1056.3

Table 17 shows computed values of ΔH_{rxn}, ΔS_{rxn} and ΔG_{rxn} with different types and basis sets for following reaction. Note that the different types of theory predict ΔS_{rxn} very consistently and in close agreement with the semi-empirical result.

Mechanism 3 (step 3):

$$Cu(NH_3)_3(OOH)^+ + HArg^+ + 2H_2O + NH_3 \rightarrow Cu(NH_3)_4(H_2O)_2^{2+} + H_2O_2 + Arg$$

Table 17. Computed Thermodynamic Properties for mechanism 3 step 3 (M3S3)

Theoretical Methods (Basis sets)	ΔH_{rxn} (kJ/mol)	ΔS_{rxn} (kJ/mol)	ΔG_{rxn} (kJ/mol k)
SE(PM3)	-172.8	-0.244	-100.08
DF(6-31G*)	-22.53	-0.244	50.182
DF(6-31G)**	-22.53	-0.244	50.182
HF (6-31G*)	-24.58	-0.245	48.13
HF (6-31G)**	-24.59	-0.245	48.13

Table 18 shows computed values of ΔH_{rxn}, ΔS_{rxn} and ΔG_{rxn} with different types and basis sets for following reaction. Note that the different types of theory predict ΔS_{rxn} very consistently and in close agreement with the semi-empirical result. This is the same step as in M1S1.

Mechanism 4 (step 1):

$$Cu(NH_3)_4(H_2O)_2^{2+} + O_2^- \rightarrow Cu(NH_3)_3(H_2O)^+ + O_2 + NH_3 + H_2O$$

Table 18. Computed Thermodynamic Properties for mechanism 4 step 1 (M4S1)

Theoretical Methods (Basis sets)	ΔH_{rxn} (kJ/mol)	ΔS_{rxn} (kJ/mol)	ΔG_{rxn} (kJ/mol k)
SE(PM3)	48.59	+0.350	-55.71
DF(6-31G*)	420.82	+0.350	316.22
DF(6-31G)**	420.87	+0.350	316.22
HF (6-31G*)	425.34	+0.350	321.04
HF (6-31G)**	425.37	+0.350	321.08

Table 19 shows computed values of ΔH_{rxn}, ΔS_{rxn} and ΔG_{rxn} with different methods and basis sets for following reaction. Note that the different types of theory predict ΔS_{rxn} very consistently and in close agreement with the semi-empirical result.

Mechanism 4 (step 2):

$$Cu(NH_3)_3(H_2O)^+ + O_2^- + H_3O^+ \rightarrow Cu(NH_3)_3(OOH)^+ + 2H_2O$$

Table 19. Computed Thermodynamic Properties for mechanism 4 step 2 (M4S2)

Theoretical Methods (Basis sets)	ΔH_{rxn} (kJ/mol)	ΔS_{rxn} (kJ/mol)	ΔG_{rxn} (kJ/mol k)
SE(PM3)	-684.98	-0.102	-654.52
DF(6-31G*)	-1035.82	-0.104	-1004.82
DF(6-31G)**	-1035.55	-0.104	-1004.82
HF (6-31G*)	-1038.21	-0.104	-1007.21
HF (6-31G)**	-1038.25	-0.104	-1007.21

Table 20 shows computed values of ΔH_{rxn}, ΔS_{rxn} and ΔG_{rxn} with different methods and basis sets for following reaction. Note that the different types of theory predict ΔS_{rxn} very consistently and in close agreement with the semi-empirical result.

Mechanism 4 (step 3):

$$Cu(NH_3)_3(OOH)^+ + HArg^+ + 2H_2O + NH_3 \rightarrow Cu(NH_3)_4(H_2O)_2^{2+} + H_2O_2 + Arg$$

Table 20. Computed Thermodynamic Properties for mechanism 4 step 3 (M4S3)

Theoretical methods (Basis sets)	ΔH_{rxn} (kJ/mol)	ΔS_{rxn} (kJ/mol)	ΔG_{rxn} (kJ/mol k)
SE(PM3)	-172.8	-0.244	-100.08
DF(6-31G*)	-22.53	-0.244	50.182
DF(6-31G)**	-22.53	-0.244	50.185
HF (6-31G*)	-24.58	-0.245	48.13
HF (6-31G)**	-24.59	-0.245	48.13

3.2.11 Computed thermodynamic properties for the overall reaction

Table 21 shows computed values of ΔH_{rxn}, ΔS_{rxn} and ΔG_{rxn} with different methods and basis sets for all four mechanisms. Note that the different types of theory predict ΔS_{rxn} very consistently and in close agreement with the semi-empirical result.

Table 21. Computed Thermodynamic Properties for the overall reaction using $HArg^+$ and H_3O^+ , which are the same for all four mechanisms.

Theoretical methods (Basis sets)	ΔH_{rxn} (kJ/mol)	ΔS_{rxn} (kJ/mol)	ΔG_{rxn} (kJ/mol k)
SE(PM3)	-809.2	0.004	-810.52
DF(6-31G*)	-637.9	0.002	-638.52
DF(6-31G)**	-637.85	0.002	-638.95
HF (6-31G*)	-639.52	0.001	-640.52
HF (6-31G)**	-639.52	0.001	-640.59

It is remarkable that both the density functional and Hartree-Fock methods give similar results for all electron mechanistic steps and hence overall reactions. The semi-empirical method gives more –ΔG's for two out of three steps for each mechanism, and more –ΔG's for the overall reaction. This is the same table as four, calculated separately for the mechanisms, but resulting in the same overall reaction.

3.3 BUILDING AND LOCATING TRANSITION STATES

We used the Spartan 2004* procedure for building and locating transition states. The software helps in providing both an extensive and extendable library of calculated transition states, and a facility for matching as nearly as possible entries in the library with the given reaction. If the reaction is unknown to library, as in our cases a fall back technique is automatically invoked in the program which is similar to the "linear synchronous transit" method to give average geometries of the intermediate transition states. According to this method a structure in between reactants and products is selected, and the electron flow from bonds being broken to bonds being formed is programmed. A maximum of the potential energy along this reaction coordinate in selected and this structure motion corresponds to an imaginary vibrational frequency, also known as the reaction coordinate. All other normal modes behave as usual as harmonic oscillators with real frequencies of vibration.

Our attempts to model transition state with HF and DF methods proved very time consuming and subject to frequent failures to converge to stable values. We could only meet these requirements using PM3. One reason for these difficulties is the much larger number of electrons for the Cu^{2+} used in the intermediates, and another may have been the false "maxima" found along incorrect pathways.

When the mechanistic steps are connected, new reactants are usually added to the products of previous reaction, which adds enthalpy to the reactants of the current reaction. We refer to this as "reorganization energy," which effectively adds to the barriers slowing down the reaction. The normal driving force is due to the negative activation energies always found for the transition states relative to their reactants. This is anticipated in the case of charge transfer reactions, which are usually taken to have zero activation energy. A schematic summary of these effects is given in Figure 3 as follows.

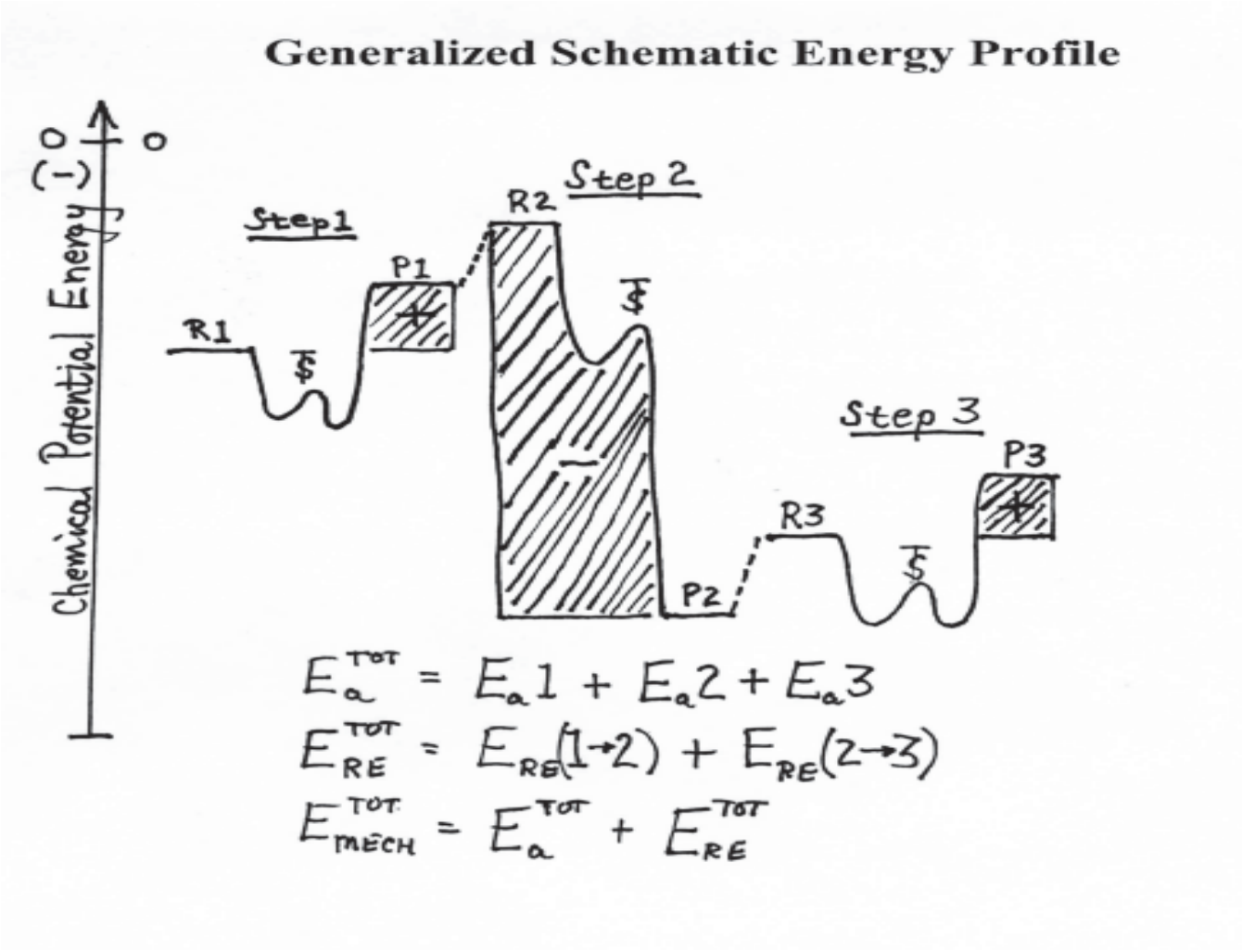

Figure 3 Schematic generalized energy profile for a three step mechanism showing the negative activation energies and reorganization energies that effect the driving forces (-) and barriers (+) to the overall reaction as measured by E_{mech}

3.3.1 Activation, reorganization and net energies for all the four mechanisms

Table 22 shows computed values of ΔH of formation of reactants, transition state, reorganization, net and activation energies at semi-empirical (PM3).

Table 22. Activation, reorganization and net energies for all the four mechanisms (kcal/mol)

Level of theory PM3	ΔH of reactants	ΔH of transition state	Activation Energy (E_a)	Reorganization Energy	Net Energy
Mechanism 1: Step 1	-34	-200.2	-166.2		
Step 2	-104	-134	-238	271.8	-119.0
Mechanism 2: Step 1	-34.5	-127.0	-92.5		
Step 2	46.3	19.6	-19.6	86.7	
Step 3	-146.9	-135.4	-282.3	184.2	-122.3
Mechanism 3: Step 1	-34.5	-127.0	-92.5		
Step 2	119.0	25.3	-93.9	251.2	
Step 3	-66.5	-145.5	-79.2	-68.1	-91.5
Mechanism: 4 Step 1	-34	-200.2	-166.2		
Step 2	1905	35.7	-16.2	202.5	
Step 3	-66.2	-148.1	-82.1	-69.2	-92.2

4. CONCLUSIONS AND FUTURE DIRECTIONS

In an attempt to model the active site dismutation of superoxide with Cu^{2+}/Cu^{+}, we investigated the thermodynamics and kinetics of four mechanisms. The thermodynamic values were checked against overall reaction values, we found good agreement with the different levels of theory and basis sets. The net energy released by each mechanism is a measure of the absence of a barrier to the overall dismutation reaction. Table 22 shows that both mechanisms 1 and 2 as previously suggested are more likely in this sense. This argues against a peroxy ($^{\cdot}OOH$) intermediate (mechanisms 3 and 4), and the possible presence of the unusual neutral species, [Cu $(NH_3)_3(O_2)$] in mechanism 2.

Future directions should include a using higher level basis set and the Ohio computer in searching for transition state. The current thermodynamics are well in hand. The treatment of such redox biocatalysts involving electron transfer needs more attention to the formalism by which exothermic reactions have transition state energies less than the reactants.

5. BIBILIOGRAPHY

1. Leach, A.R., "Molecular Modeling: Principles and Applications, "2nd ed., Pearson Prentice Hall, Harlow, England; **2001.**
2. Tinoco, I.; Sauer, K.; Wang, J.C. "Physical Chemistry, "2nd.ed. Prentice Hall, Englewood Cliffs, NJ; **1985.**
3. Niviere, V. and Fontecave, M. *J. Biol. Inorg. chem*.**2004,** 9(2), 119-23.
4. Ciriolo, M.R.; Battisoni, A.; Falconi, M.; Filomeni, G; Rotilio, G. *Eur. J. Biochem.* **2001, *268*,** 737-742.
5. Hiroyuki, U. Assay of Enzyme Superoxide Dismutase, *Dojindo Newsletter Vol 3*.
6. *http:// WWW.dojindo.com/newsletter/review vol 3-3. html*. (accessed 03-20-2005).
7. Carloni, P.T; Blichl, P.E; Parinello, M. *J. phys.Chem*. **1995,** *99*, 1338-1348.
8. Hehre, W.J; Deppmeier, B.J; Klunzinger, P.E. A *PC Spartan Tutorial*, Wave function, Inc; **1999**.
9. Vladimir, P; Siegbahn, E. M. *Inorg. Chem*. 2005; 44, 3311-3320.
10. Rosi, M.; Sgamelloti, A; Tarantelli, F; Bertini, I; Luchinat, C. *inorg. Chem*. *Acta*, **1985**,107, 21.
11. Rosi, M.; Sgamelloti, A; Tarantelli, F; Bertini, I; Luchinat, C. *inorg. Chem*. **1986**, 25, 1005.
12. Stewart, J. P. J. computational chem. **1989**, *10*, 209-220.
13. Hehre, W. J, Stewart, R.F. and People, *J.A.J. Chem. Phys*.1996, 51, 2657.
14. Hehre,W, J.; Radom, L.; Schleyer,P.V.R.; People,J.A. *Ab Initio Molecular Orbital theory*, John Wiley & Sons, Inc.; **1986.**
15. Hehre, W.J.; Ditchfield, R. and people, J. A. *J. Chem. Phys*. **1972**,56,2257.

16. Binkley, J.S.; People, J.A. and Hehre, W.J. *J. Chem. Soc*. **1980**. 102, 939.

17. Hariharan, P.C. and people, J. A. *Chem. Phys. Lett*. **1972**, 66, 217.

18. Parr, R.G. and Yang, W. *Density Functional Theory of Atoms and molecules,* Oxford Univ. Press, **1989**.

19. Pederson, T. B. www. Fysik.dtu.dk/ Bligaard/ms/ node8.html, (accessed 01-29-2005).

20. Leach, A.R. *Molecular modeling- Principles and Applications*, Pearson Education Limited Second edition; **2001**.

21. Worthington Biochemical Corporation. *http;//www.worthington-biochem.com/ SODBE/ default. html*, (accessed 04- 18-2005).

22. Chase, M.W. NIST-JANAF Thermochemical tables, *Amer.Inst.Phys.* and Amer. *J. Chem. Soc*. **1998**.

23. Martin, S.; Michal, P.; Pavel, N. and Miroslav, U. *Int. J. Quantum. Chem.* **2008,** 108, 2159.

24. James, A.F. and Christopher, B. *J. Biol. Chem.* **1986,** 261, 13000.

25. Andrea, B.; Silvia, F.; Laura, C.; Francesca, P.; Alessandro, D.; Anna, G. and Gluseppe, R. *J. Biol. Chem.* **1998,** 273, 5655.

26. Norihide, S.; Kazuo, K. and Koichiro, H. *J.Biol. Chem.* **1983,** 259, 4414.

27. McCord, M. and Irwin, F. *J. Biol .Chem.* **1969,** 244, 6049.

28. Adam, T. F.; Peter, B.; Michael, J.M. and Thomas, C. B. *J. Am.Chem. Soc.* **2005,** 127, 5462.

29. Suranjan, B. C.; Gerard, D.; Manju, S.; Diane, E. C. and Michael, J. M. *J. Biochem.* **1999,** 38, 3744.

30. Jian, Li.; Cindy, L. F.; Robert, K. Donald, B. and Louis, N. *J. Inorg. Chem.* **1999,** 38, 929.